WORLD SPINE JOURNAL
WSJ. 2006;1(2):68-73 Volume 1: Issue 2

# Evaluating Atlantoaxial Anatomy and Screw Placement with Three-Dimensional Cone-Beam Computed Tomography

Doron Rabin, MD[1]; David McErlain, MSc[2]; DW Holdsworth, PhD[2]; David Pelz, MD[3]; Ramesh Sahjpaul, MD[4]; Neil Duggal, MD[1]

[1]Division of Neurosurgery, University of Western Ontario
[2]Department of Medical Biophysics, John P. Robarts Research Institute, University of Western Ontario
[3]-Department of Diagnostic Radiology and Nuclear Medicine, University of Western Ontario, Neuroradiology Section, London Health Sciences Centre
[4]Division of Neurosurgery, University of British Columbia

**Acknowledgements** The authors thank Chris Norley for his help in preparation of the manuscript.

**Abstract**

Objective: Accurate imaging of atlantoaxial disorders is essential to patient selection, intraoperative management and postoperative assessment of screw placement. We describe the first application of the C-arm mounted Siemens Multistar Image Intensifier cone-beam computed tomography (CT) system in the surgical management of atlantoaxial disorders.

Materials and Methods: Pre- and postoperative imaging using the Siemens Multistar system and conventional helical CT imaging was performed to evaluate six patients requiring either transarticular C1-2 or odontoid screw fixation. The accuracy of the Siemens Multistar system was compared with conventional helical CT with respect to perioperative clinical utility.

Results: Two odontoid and six transarticular screws were placed in six patients. Preoperative and postoperative cone-beam CT techniques allowed reconstruction of 3-D images for the evaluation of Type II odontoid fractures and the anatomic suitability of the atlantoaxial complex for transarticular screw fixation. Postoperative cone-beam CT imaging demonstrated accuracy of screw placement and extent of fracture reduction. Radiation exposure for preoperative and postoperative imaging using cone-beam CT were 0.049 mSv (SD 0.026 mSv) and 0.098 mSv (SD 0.026 mSv), respectively.

Conclusions: Three-dimensional fluoroscopy using cone-beam 3-D CT techniques with the Siemens Multistar Intensifier provided clinically useful images in the perioperative assessment of atlantoaxial disorders. Potential advantages of cone-beam CT include reduced radiation dose, rapid acquisition times and possible intra-operative applications, including real-time 3-D image guidance.

Key words: computed tomography, transarticular screw, odontoid screw, atlantoaxial disorders, three-dimensional fluoroscopy

## Introduction

Accurate placement of transarticular C1-2 and odontoid screw fixation requires precise pre- and intraoperative imaging. Preoperative imaging with computed tomography (CT) is essential for evaluation of regional anatomy, fracture morphology and overall patient selection for both odontoid and C1-2 transarticular screw placement.(1-7) Careful evaluation of variant anatomy can prevent intraoperative complications, such as vertebral artery and spinal cord injury.(1,4,5,7-12) Standard operative techniques for both transarticular and odontoid screw procedures rely on anatomic landmarks and intraoperative fluoroscopy to guide screw trajectory.(3,4,8) Although fluoroscopy improves accuracy and reduces surgical exposure, it is limited by providing only a single real-time planar view. For procedures like odontoid screw insertion, multiplanar fluoroscopic visualization is required either with two mobile C-arm fluoroscopes or tedious repositioning of a single C-arm. Image-guided surgery (IGS) has improved the accuracy of C1-2 transarticular screw placement by allowing the surgeon to navigate the relevant anatomy of axis.(13) Ideally, however, intraoperative imaging should provide real-time imaging of atlantoaxial relationship with CT-like quality images.

**Figure 1.** Modified Siemens Multistar rotational angiography prototype; the X-ray tube is located at the top position of the C-arm, X-ray image intensifier (XRII) is seen below. The C-arm rotates over 200° with a speed of 45° per second making acquisition times as low as 4.4 seconds.

The Siemens Multistar Image Intensifier (XRII) (Siemens Medical Systems, Erlangen, Germany) is a 3-D C-arm fluoroscopy unit that allows 200° of rotation around the patient. In several seconds, it acquires images for rapid reconstruction into detailed coronal, axial and sagittal views of relevant anatomy, comparable to images produced by a CT scanner. With specialized software, the acquired images can be used to generate 3-D images, which can be rotated and manipulated to provide detailed visualization of anatomy, pathology and therapeutic interventions. We describe our initial experience with the Siemens Multistar Image Intensifier (XRII) for perioperative evaluation of the atlantoaxial complex.

## Methods and Materials

In this limited prospective cohort, six patients presenting with atlantoaxial instability were evaluated with conventional static and dynamic cervical plain films and a helical CT system to determine their suitability for surgery. For patients requiring either transarticular or odontoid screw surgery, informed consent was obtained for additional preoperative and postoperative imaging using the Siemens Multistar system. Two investigators (ND and RS) compared the quality of images obtained with the conventional helical CT system and the Siemens Multistar X-ray Image Intensifier (XRII) CT system. Images were compared based on accuracy of preoperative anatomy and placement of instrumentation.

The application of the Siemens Multistar rotational prototype cone-beam CT system has been previously described for the production of 3-D neurovascular images.(14) The X-ray source and XRII are mounted at opposite ends of the C-arm (**Figure 1**) and rotate approximately 200° around the patient's head and cervical spine at a speed of 45° per second. The X-ray "slices" are acquired at 1.5° intervals at a rate of up to 30 frames per second, resulting in 130, 512 x 512 images over 200°. Total image acquisition time was 4.4 seconds. The maximum field of view the system achieves is 40 cm.

The images were reconstructed using a Feldkamp cone-beam reconstruction algorithm.(15) The methods used to correct for non-linear motion of the C-arm in the circular path and distortion caused by the XRII are described elsewhere.(16-18) Each image was digitized in 440 X 440 pixel format (with pixel sizes of 0.379 mm and 0.30 mm for the 28 cm and 20 cm fields of view respectively). The scans using a 28 cm field of view produced a data cube with dimensions of 15 x 15 x 15 cm cubed with 0.5 mm isotropic voxel spacing. The 20 cm field of view created a data cube with dimensions of 13 x 13 x 13 cm cubed with 0.5 mm isotropic voxel spacing. The volumes were viewed at a workstation in various forms, including a surface rendering (**Figure 1**), a maximum intensity projection (MIP) and a visual file format (VFF) (**Figure 2**).

## Results

**Clinical:** Patients were scanned with helical and XRII pre- and postoperatively. Two patients presented with a Type II odontoid fracture requiring placement of an odontoid screw. Preoperative helical and XRII CT were used to evaluate the fracture site, the displacement of the odontoid peg and the anatomy of the C1-2 complex. Sagittal reconstructions were

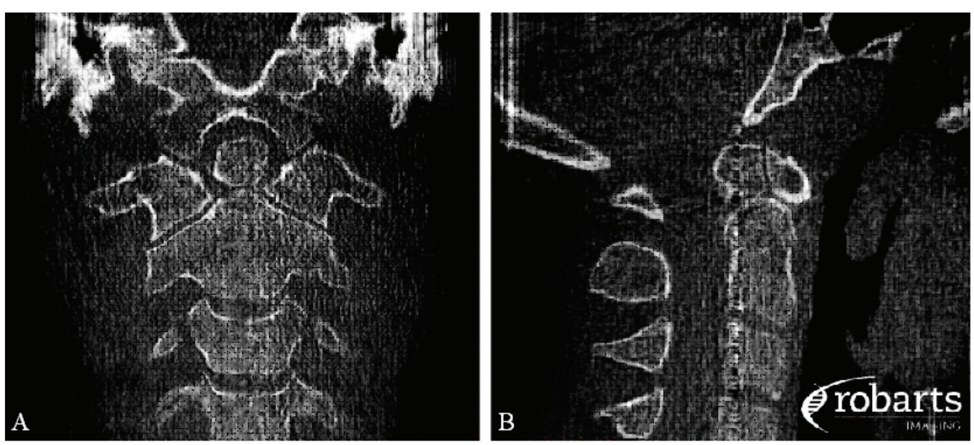


**Figure 2.** C-arm mounted XRII CT images of cervical spine: (a) coronal and (b) sagittal views.

used for planning the trajectory of screw placement. Postoperative helical and XRII CT demonstrated acceptable screw placement in both patients. The remaining four patients presented with C1-C2 instability of varying etiologies. Preoperative helical and XRII CT images were equally useful in the clinical evaluation of relevant anatomy, including the size of the pars interarticularis. Intraoperative conventional single-planar C-arm fluoroscopy and image guidance were used at the time of surgery. Postoperative helical and XRII CT imaging were felt to be equivalent in demonstrating screw placement in all cases. A total of six transarticular screws (two bilateral; two unilateral) were placed. Detailed patient information is presented in **Table 1**.

**Imaging:** Four patients were scanned with a 28 cm field of view, while the remaining two were scanned using 20 cm field of view to enlarge the view of the atlantoaxial joint. A summary of the imaging parameters for each patient is provided in **Table 2**. The section thickness in each volume was 0.5 mm with the XRII system versus a 1 mm for the helical CT scanner. Image quality for axial, coronal and sagittal images was comparable between helical and XRII CT.

The XRII system scans produced over 200 two-dimensional projections needed to reconstruct the data into a 3-D volume. The tube voltage varied between 90 and 125 kV, and the tube current ranged from 141 to 380 mA. The exposure time per frame was between 3 and 6 msec. The Siemens Multistar system exposed patients to a mean radiation dose of 0.049 mSv (SD 0.026 mSv) for preoperative imaging and 0.098 mSv (SD 0.026 mSv) for postoperative imaging. In contrast, the helical CT exposed patients to a mean dose of 1.46 mSv of radiation.

## Discussion

Three-dimensional C-arm fluoroscopy is a significant advancement in spinal imaging. The Siemens Multistar Image Intensifier (XRII) is a 3-D C-arm fluoroscopy based unit that allows 200° of rotation around the patient. Before adapting this new technology in our operating room suite, we used this pilot study to compare imaging between 3-D fluoroscopy (cone-beam) to helical CT. Our results suggest that the imaging quality, acquisition time and radiation exposure of 3-D fluoroscopy is comparable or improved over helical CT.

### Preoperative Assessment

Three-dimensional fluoroscopy is particularly well suited for preoperative assessment of bony and vascular anatomy of the atlantoaxial complex. Variant anatomy can result in intraoperative complications, such as vertebral artery and spinal cord injury during C1-2 transarticular screw and odontoid screw procedures.(1,4,5,7-12) Solanki et al reported poor correlation between the left and right pars interarticularis with respect to morphological parameters and vertebral groove dimensions in 50 dry C2 specimens.(1) Eleven specimens (22%) were found to be inadequate for transarticular screw fixation (seven left side, three bilaterally and one right side).(1) In a retrospective study, Paramore et al reported that 17 of 94 patients (18%) receiving thin-slice antlantoaxial CT imaging for investigation of cervical trauma demonstrated unacceptable anatomy for transarticular screw placement (nine left side, five right side and three bilaterally).(4) As shown in **Figure 2**, the 3-D fluoroscopy images are comparable in quality to those seen in helical CT. It also has the capability of delineating vascular anatomy as demonstrated in pig models and human skull phantoms.(14)

In cases of spinal instability, particularly those resulting from trauma, inflammatory processes or neoplasm, the intersegmental relationship between C1 and C2, after intraoperative positioning, can differ from preoperative imaging. Conventional image guidance is limited in outlining only the anatomy of C2. It is unable to accurately demonstrate

**Table 1.** Patient characteristics.

| | Age/Gender | Etiology | Procedure |
|---|---|---|---|
| 1 | 86/f | Type II odontoid fracture | Closed reduction and odontoid screw fixation |
| 2 | 74/m | Type II odontoid fracture traversing the left arches and lateral mass of C1 | Closed reduction and odontoid screw fixation |
| 3 | 22/f | Os odontoideum | C1-C2 transarticular screw placement and C1-C2 autograft secured with interlaminal wire |
| 4 | 46/f | C1-C2 rotational subluxation resulting in vertebrobasilar insufficiency | C1-C2 transarticular screw fixation and C1-C2 autograft secured with interlaminar wiring |
| 5 | 18/m | C1-C2 subluxation following right lateral mass fracture extending into the foramen transversarium | Right C1-C2 transarticular screw fixation with C1 partial laminectomy and left interlaminar C1-C2 autograft secured with interlaminar wiring |
| 6 | 36/f | C1-C2 rotational subluxation following C1 laminectomy and suboccipital decompression | Left C1-C2 transarticular screw fixation |

**Table 2.** Imaging parameters and X-ray dose of C-arm mounted XRII cone-beam CT system.

| Patient | | Volt (kV) | Current (mA) | Time (msec) | X-ray dose (mSv) |
|---|---|---|---|---|---|
| 1 | Preoperative | 90 | 234.3 | 3 | 0.045 |
| 2 | Preoperative | 90 | 140.6 | 3 | 0.027 |
| 3 | Preoperative | 90 | 380 | 3 | 0.082 |
| | Postoperative | 125 | 223.8 | 6 | N/A |
| 4 | Preoperative | 90 | 209 | 3 | 0.039 |
| | Postoperative | 90 | 329.8 | 5 | 0.12 |
| 5 | Preoperative | 125 | 241.8 | 5 | N/A |
| | Postoperative | 90 | 356 | 5 | 0.12 |
| 6 | Preoperative | 90 | 307.6 | 6 | 0.087 |
| | Postoperative | 90 | 329.8 | 5 | 0.070 |

kV - kilovolts, mA - millliamperes, msec - milliseconds, msv - millisieverts

the relationship between C1 and C2. Three-dimensinoal fluoroscopy avoids potential inaccuracies from positioning or intraoperative manipulation. After positioning or reduction, a data set is acquired which demonstrates the intraoperative relationship between C1 and C2. With odontoid fractures, especially in cases of osteoporosis, it can be difficult to judge the degree of open or closed reduction. Three-dimensional fluoroscopy can be used to guide open and close reduction as well as screw placement.

## Radiation Exposure

The Siemens Multistar system exposed patients to a mean dose of 0.049 mSv (SD 0.026 mSv) for preoperative imaging and 0.098 mSv (SD 0.026 mSv) for postoperative imaging. Slomczykowski et al compared the radiation dose administered during fluoroscopy-guided lumbar pedicle screw insertion and CT-based computer assisted surgery.(19) Anthropomorphic phantoms were exposed to 1.0 mSv of radiation in order to simulate the insertion of six pedicle screws with a fluoroscopy time of 63 seconds for each screw.(19) This corresponds to a dose of 0.17 mSv per screw inserted. The same authors reported that preoperative CT imaging for computer assisted pedicle screw insertion resulted in much higher radiation exposures.(19) Sequential CT, optimized spiral CT and optimized sequential CT imaging protocols resulted in effective exposures of 4.1 mSv, 3.0 mSV and 2.4 mSv respectively.(19) The Siemens Multistar system used in this study provided imaging of comparable quality to contemporary CT protocols with less radiation exposure.

## Intraoperative Applications

Placement of a screw within the atlantoaxial complex demands a high level of accuracy.(20) Poor surgical outcomes (eg, nonunion and/or continued instability) may result from inadequate reduction of the fracture or suboptimal hardware placement.(8) Rampersaud et al used a pedicle model based on morphometric data to determine maximal deviations from optimal pedicle screw trajectory that would not perforate the pedicle wall.(21) The maximum acceptable translational placement error for 3.5 mm C2 pedicle screws was reported as 1.7 mm assuming zero rotational error.(21) Maximum rotational error for 3.5 mm C2 pedicle screws was 6.10 with a no translational error.(21) This resulted in a relative combined error estimate of approximately 50/mm.(21) Similarly, optimal odontoid fracture reduction is essential to minimizing the potential for instrumentation complications secondary to anterior screw insertion.(7,20) Subach et al reported that 3% of odontoid screws were malpositioned after reviewing 252 cases of odontoid fixations reported in the literature.(7)

Standard operative technique for both transarticular and odontoid screw procedures relies on anatomic landmarks and intraoperative fluoroscopy to guide screw trajectory.(2,3,8) Xu et al demonstrated that 50% of C1-C2 transarticular screws set to underpenetrate the lateral mass of C1

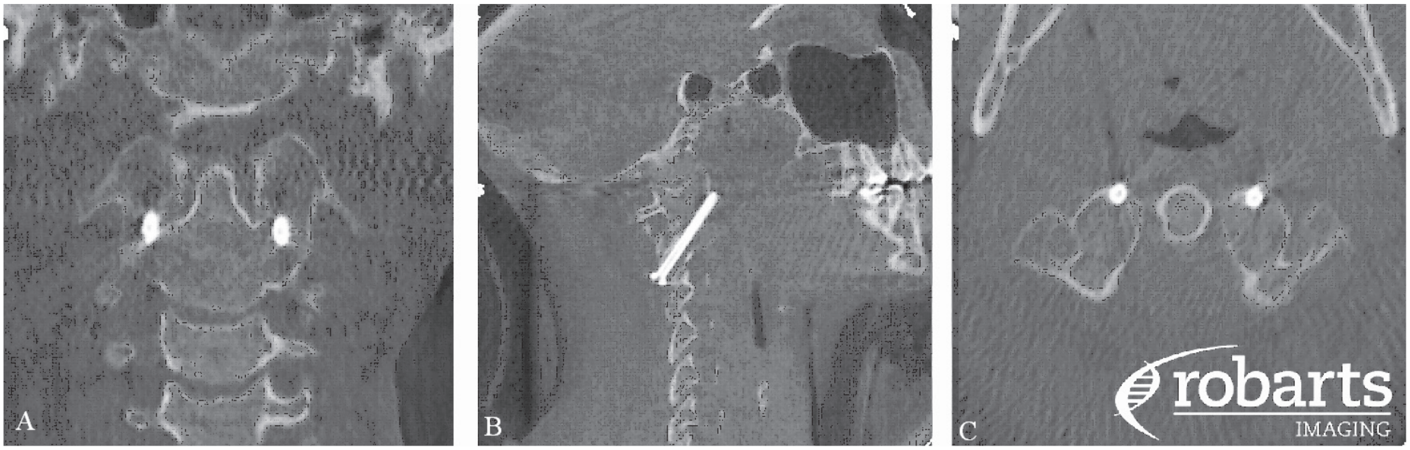


**Figure 3.** Coronal (A), sagittal (B) and axial (C) postoperative XRII cone-beam CT images of the cervical spine with C1-C2 transarticular screws in place.

were projected in the middle region of the odontoid process on lateral radiograph.(8) Fifty percent of the C1-C2 transarticular screws set to overpenetrate the ventral cortex of the lateral mass projected on the anterior region of the odontoid on lateral radiographs.(8) Based on these findings the authors concluded that lateral radiographs were not reliable in determining optimal screw length.(8)

The Siemens Multistar system can produce 3-D volumes with real CT attenuation numbers in Hounsfield units. With new software development and use of a workstation designed solely for processing these images, 3-D images of the screw placement relative to the vertebral column can be readily acquired (**Figure 3, 4 & 5**). The potential benefits of intraoperative 3-D fluoroscopy are numerous. In the operating room, it can acquire data to generate 3-D reconstructed images, thereby avoiding potential inaccuracies in intervertebral alignment that can occur between preoperative imaging and intraoperative positioning. In cases where a decompression or reconstruction of the spine is performed, 3-D fluoroscopy provides detailed imaging of bony structures. This may be especially useful to evaluate the thoroughness of decompressive procedures. In cases where spinal fixation is used, a postoperative scan can be performed in the operating room to ensure the accuracy of the internal fixation. A receiver operating characteristics study of the Siemens Isocentric Mobile C-Arm (Iso-C) (Siemens Medical Solutions, Enlargen, Germany) indicated that imaging of the facial skeleton revealed no difference in sensitivity and specificity in comparison to conventional helical CT.(22) Hott et al recently reported that screw position and cortical wall violation on postoperative imaging of the spine with the Siemens Iso-C was concordant with postoperative helical CT imaging.(23) The authors felt that postoperative Iso-C images were of sufficient quality to dispense with postoperative helical CT imaging.(23)

Current efforts to optimize hardware placement focus on frameless stereotactic procedures based on preoperative CT imaging.(13, 24-28) The ideal application of 3-D fluoroscopy has been used in conjunction with image-guided spinal technology.

It can effectively function as an intraoperative CT scanner, thereby avoiding the need for a preoperative CT with an image guidance protocol and saving the added cost and time from the preoperative work-up. Open registration of the vertebral body, which can be time consuming and difficult at times, is no longer required for image guidance. This facilitates minimally invasive procedures such as percutaneous screw placement. It also allows for improved applications of image guidance for surgery involving the anterior vertebral column, where selecting anatomic landmarks for registration can be difficult. Hott et al demonstrated these advantages while using an Iso-C based neuronavigation system in 60 craniospinal surgery cases.(23) The system allowed for real-time intraoperative feedback regarding extent of resection of fibrodysplastic lesions at the skull base and positioning of instrumentation in the cervical, thoracic and lumbar spine.(24) The technology was successfully applied to anterior, posterior, transthoracic and percutaneous approaches to the spinal column.(23)

## Conclusions

The results of this preliminary case study support the utility of the XRII C-arm CT system in assessing preoperative atlantoaxial anatomy and postoperative fracture reductions and hardware placement. Anticipated incorporation of this technology into the operating room may provide improved

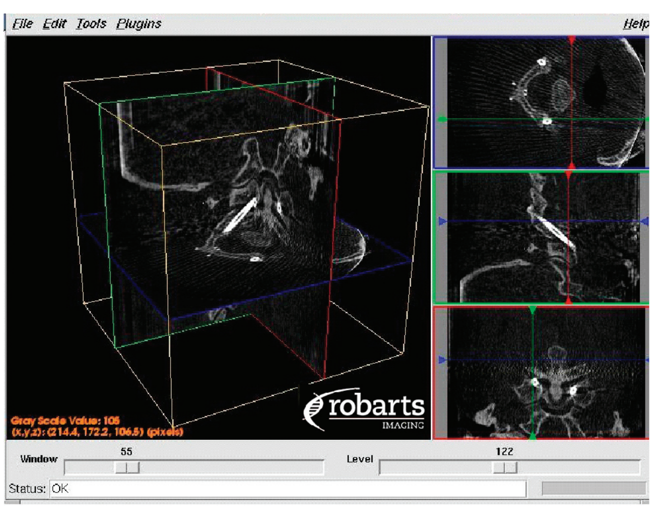


**Figure 4.** Three-dimensional volumes of XRII based cone-beam CT images of C1-C2 transarticular screws. Viewed as vff using MicroView software (GE Medical Systems, London, Canada).


**Figure 5.** Surface rendering of XRII based cone-beam CT images of C1-C2 transarticular screws.

intraoperative evaluation anatomy and hardware placement.

## References

1. Solanki GA, Crockard HA. Peroperative determination of safe superior transarticular screw trajectory through the lateral mass. Spine 1999; 24: 1477-82.
2. Fuji T, Oda T, Kato T et al. Accuracy of atlantoaxial transarticular screw insertion. Spine 2000; 24: 1760-4.
3. Haid WH. C1-C2 transarticular screw fixation: technical aspects. Neurosurgery 2001; 49: 71-4.
4. Paramore CG, Dickman CA, Sonntag VKH. The anatomical suitability of the C1-2 complex for transarticular screw fixation. J Neurosurg 1996; 85: 221-4.
5. Madawi AA, Casey ATH, Solanki GA, et al. Radiological anatomical evaluation of atlantoaxial transarticular screw fixation technique. J Neurosurg 1997; 86: 961-8.
6. Heller JG, Alson MD, Schaffler MB, et al. Quantitative internal dens morphology. Spine 1992; 17: 861-6.
7. Subach BR, Morone MA, Haid RW Jr, et al. Management of acute odontoid fractures with single screw anterior fixation. Neurosurgery 1999; 45: 812-20.
8. Xu R, Ebraheim NA, Misson JR, et al. The reliability of the lateral radiograph in determination of the optimal transarticular screw length. Spine 1998; 23: 2190-4.
9. Millgram MA, Rand N. Cervical spine anatomy. Spine: State of the Art Reviews. 2000; 14(3):521-34.
10. Abou-Madawi A, Solanki G, Casey AT, et al. Variation of the groove in the axis vertebra for the vertebral artery: Implications for instrumentation. J Bone Joint Surg 1997; 79B:820-3.
11. Ebraheim NA, Xu R, Yeasting RA. The location of the vertebral artery foramen and its relation to posterior lateral mass screw fixation. Spine 1996; 21:1291-5.
12. Lu J, Ebraheim NA, Yang H, et al. Anatomic considerations of anterior transarticular screw fixation for atlantoaxial instability. Spine 1998; 23:1229-35.
13. Foley KT, Simon DA, Rampersaud YR. Virtual fluoroscopy: computer-assisted fluoroscopic navigation. Spine 2001; 26: 347-51.
14. Fahrig R, Fox J, Lownie S, et al. Use of a C-Arm System to Generate True Three-dimensional Computed Rotational Angiograms: Preliminary In Vitro and In Vivo Results. AJNR Am J Neuroradiol 1997; 18:1507-14.
15. Feldkamp LA, David LC, Kress JW. Practical cone-beam algorithm. J Opt Soc Am 1984; 1:612-9.
16. Fahrig R, Holdsworth DW. Three-dimensional computed tomographic using a C-arm mounted XRII: image-based correction of gantry motion nonidealities. Medl Phys 2000; 27:30-8.
17. Fahrig R, Moreau M, Holdsworth DW. Three-dimensional computed tomographic reconstruction using a C-arm mounted XRII: correction of image intensifier distortion. Med Phys. 1997; 24:1097-1106.
18. Fahrig R, Holdsworth DW, Fox AJ. Characterization of a C-arm mounted XRII for three-dimensional image reconstruction during interventional neuroradiology. Proc SPIE 1996; 2708:351-60.
19. Slomczykowski M, Roberto M, Schneeberger P, et al. Radiation dose for pedicle screw insertion fluoroscopic method versus computer assisted surgery. Spine 1999; 24: 975-83.
20. McLain RF. Salvage of a malpositioned anterior odontoid screw. Spine 2001; 26: 2381-4.
21. Rampersaud YR, Simon DA, Foley KT. Accuracy requirements for image-guided spinal pedicle screw placement. Spine. 2001; 26: 352-9.
22. Heiland M, Schulze D, Adam G, et al. 3-D-imaging of the facial skeleton with an isocentric mobile C-arm system (Siremobil Iso-C). Dentomaxillofac Radiology. 2003; 32: 21-5.
23. Hott JS, Deshmukh VR, Klopfenstein JD, et al. Intraoperative iso-c c-arm navigation in Craniospinal surgery: the first 60 cases. Neurosurgery 2004; 54; 1131-1137.
24. Welch WC, Subach BR, Pollack IF, et al. Frameless stereotactic guidance for surgery of the upper cervical spine. Neurosurgery 1997; 40: 958-64.
25. Kawaguchi Y, Ishihara H, Ohmori K, et al. Computer-assisted Magerl's transarticular screw fixation for atlantoaxial subluxation. J Orthop Sci 2002; 7(1): 131-6.
26. Cleynenbreugel J, Schutyser F, Goffin J, et al. Image-based planning and validation of C1-C2 transarticular screw fixation using personalized drill guides. Comput Aided Surg 2002; 7(1): 41-8.
27. Goffin J, Van Brussel K, Martens K, et al. Three-dimensional computed tomographic-based personalized drill guide for posterior cervical stabilization at C1-C2. Spine 2001; 26(12): 1343-7.
28. Weidner A, Wahler M, Chiu ST, et al. Modifications of C1-C2 transarticular screw fixation by image-guided surgery. Spine 2000; 25(20): 2668-73.